JOURNAL OF SOLID STATE CHEMISTRY 114, 539–542 (1995)

$T(z)$ Diagram and Optical Energy Gap Values of $(AgIn)_{2(1-z)}(MnIn_2)_zTe_4$ Alloys

R. Cadenas

Departamento de Física, Universidad del Zulia, Maracaibo, Venezuela

and

M. Quintero and J. C. Woolley[1]

Centro de Estudios de Semiconductores, Departamento de Física, Universidad de Los Andes, Mérida, Venezuela

Received January 10, 1994; in revised form June 3, 1994; accepted June 13, 1994

The $T(z)$ diagram of the system $(AgIn)_{2(1-z)}(MnIn_2)_zTe_4$ was obtained from X-ray powder diffraction and differential thermal analysis measurements. At high temperatures, there is a single-phase solid solution across the complete diagram in a disordered defect zinc-blende phase β. This β phase shows a eutectoid reaction at $z = 0.63$ and $T = 465$°C giving the two tetragonal terminal phases α, $AgInTe_2$, and γ, $MnIn_2Te_4$, of space groups $I\bar{4}2d$ and $I\bar{4}2m$ respectively. At lower temperatures, the fields α and γ are separated by a relatively wide two-phase field ($\alpha + \gamma$) which extends over the range $0.52 < z < 0.78$. Values of room-temperature optical energy gap E_0 were determined from optical absorption measurements in the ranges of single-phase behavior, and the form of the E_0 vs z data curve is discussed. The form of this $T(z)$ diagram is compared with those of related systems in which the terminal compounds have similar structure but differ in space group. © 1995 Academic Press, Inc.

INTRODUCTION

Semiconductor materials containing manganese are of interest because of the manner in which the magnetic behavior associated with the manganese can modify and complement the semiconductor properties (1, 2). It has been found that adamantine compounds with tetrahedral coordination can accept a large amount of manganese in cation substitutional solid solution. Well-known examples of such materials are the alloys based on the II–VI compounds, e.g., $Cd_{1-z}Mn_zTe$ (1). Similar alloys can be obtained by introducing manganese into the equivalent ternary compounds, the tetrahedrally coordinated I–III–VI_2 chalcopyrites, e.g., $AgInTe_2$. One way of introducing Mn into these chalcopyrites is to form the alloys with MnTe, e.g., $(AgIn)_{1-z}Mn_{2z}Te_2$, and these alloys have been investigated in some detail (3–5). However, another group of compounds that show the tetrahedrally bonded form and contain Mn are the Mn–III_2–VI_4 compounds, e.g., $MnIn_2Te_4$, which have a defect $I\bar{4}2m$ tetragonal structure closely related to the $I\bar{4}2d$ structure of the chalcopyrites. These compounds have received some attention (e.g., (6, 7)), but much less than the chalcopyrites, and recently alloy systems between these and the corresponding non-magnetic compounds, e.g., $CdIn_2Te_4$, have been studied (8–10). Because of the similarity of the two structures, it appeared probable that appreciable solid solution would occur between compounds of these types, and in the present work, the $T(z)$ phase diagram of the alloy system $(AgIn)_{2(1-z)}(MnIn_2)_zTe_4$ has been investigated. In addition to the different space groups of these two compounds, another interesting difference in the cation arrangement is that while in the chalcopyrite-type $AgInTe_2$ the Ag and In atoms are fully ordered on the cation sublattice; in $MnIn_2Te_4$ the lattice vacancies are ordered on the cation sublattice but the Mn and In atoms occupy the remaining cation sites at random. It has been shown (11) for these Mn–III_2–VI_4 compounds, that those in which the Mn are disordered have very different magnetic behavior from those showing an ordered Mn arrangement.

SAMPLE PREPARATION AND EXPERIMENTAL MEASUREMENTS

Alloy samples of $(AgIn)_{2(1-z)}(MnIn_2)_zTe_4$ with various values of z were prepared by the usual melt and anneal technique (12). The components of each 1.0-g sample were sealed under vacuum in a quartz capsule, melted together at 1150°C, annealed to equilibrium at 500°C, and slowly cooled to room temperature. Previous experience indi-

[1] Permanent address: Physics Department, University of Ottawa, Ottawa, Ontario, Canada K1N 6N5.

0022-4596/95 $6.00

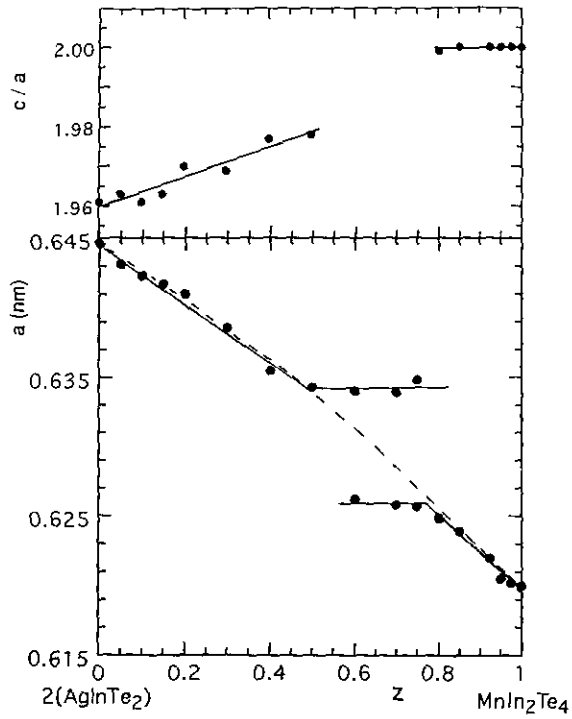

FIG. 1. Variation of lattice parameters a and c/a with composition z for the $(Ag)_{2(1-z)}(MnIn_2)_zTe_4$ alloys: (●) experimental values; (———) lines fitted to separate linear equations; (----) line fitted to quadratic equation.

cates that for this type of alloy, this procedure gives samples showing conditions corresponding to equilibrium at 200–300°C. Guinier X-ray powder photographs were used to check each sample and lattice parameter values were determined as a function of z, with germanium as the internal standard.

Transition temperatures were determined from differential thermal analysis (DTA) measurements with silver used as reference material. The charge was of powdered alloy of typical weight 50 to 100 mg. The temperatures of the sample and the reference were determined with chromel–alumel thermocouples, with the difference signal between the sample and the reference and the temperature signal being continuously recorded. For each peak in the difference signal, a phase transition temperature was determined from the baseline intercept of the tangent to the leading edge of the peak (13). Both heating and cooling runs were made, the average rates of heating and cooling being approximately 15°C/min.

Slices of each single-phase sample were cut and thinned to give specimens for optical absorption measurements by the usual method (14). Values of $\ln(I_0/I)$, where I_0 and I are, respectively, the incident and transmitted intensities, were determined as a function of photon energy $h\nu$ and corrected by subtracting a background value to give the absorption coefficient. Graphs of $(\alpha h\nu)^2$ vs $h\nu$ were then used to give values of the optical energy gap E_o.

EXPERIMENTAL RESULTS AND ANALYSIS

The X-ray photographs for the samples annealed at 500°C showed the expected form, the alloys at the $AgInTe_2$ end of the diagram having the standard chalcopyrite structure α while those close to $MnIn_2Te_4$ had a pseudocubic (zinc-blende) γ form, but with faint ordering lines indicating the tetragonal symmetry. A few alloys close to the center of the diagram clearly showed both phases. Values of lattice parameters were determined in all cases and the variations of a and c/a with z are shown in Fig. 1. The probable error in the lattice parameter values was estimated to be ±0.0005 nm. In the two single-phase regions, within the limits of experimental error, a varies linearly with z and from the a values in the two-phase region, the limits of single-phase solid solution were estimated to be $z = 0.46$ and $z = 0.78$. Straight line fits to the two linear regions gave

$$a_\alpha = 0.6446 - 0.0209\ z\ (\text{nm}) \quad R = 0.993$$

$$a_\gamma = 0.6482 - 0.0288\ z\ (\text{nm}) \quad R = 0.989$$

$$(c/a)_\alpha = 1.960 + 0.0384\ z \quad R = 0.951.$$

DTA measurements were made on each sample and the resulting $T(z)$ diagram is shown in Fig. 2, the estimated relative accuracy of the points being ±10 K. The two compounds show transition temperatures in agreement with those published previously (15, 16). Thus $AgInTe_2$

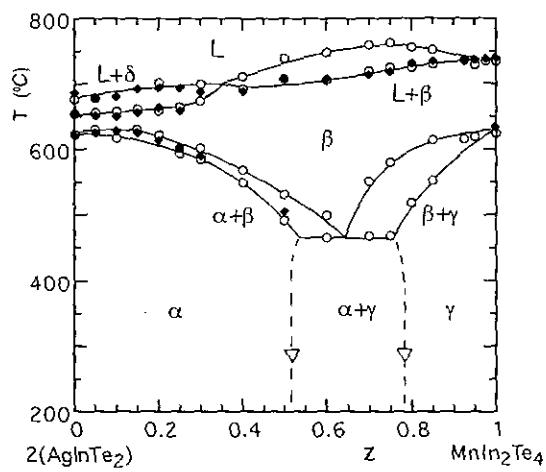

FIG. 2. $T(z)$ diagram for the $(AgIn)_{2(1-z)}(MnIn_2)_zTe_4$ alloys; (○) DTA heating run, (◆) DTA cooling run, (▽) value from lattice parameter data. α, chalcopyrite $I\bar{4}2d$ structure; β, disordered defect zinc-blende structrue; γ, ordered tetragonal $I\bar{4}2m$ structure; δ, phase with zinc-blende structure from Ag_2Te–In_2Te_3 section.

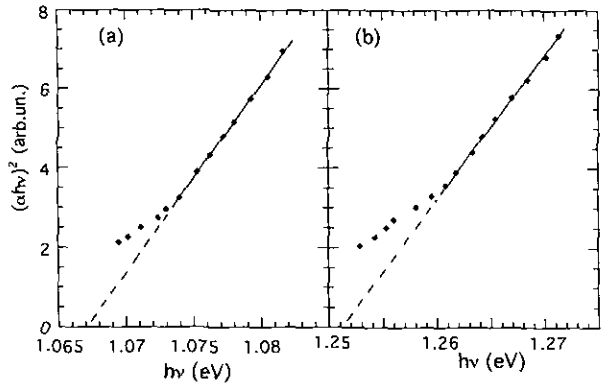

FIG. 3. Variation of $(\alpha h\nu)^2$ with $h\nu$ for representative $(AgIn)_{2(1-z)}(MnIn_2)_zTe_4$ alloys: (a) $z = 0.20$; (b) $z = 0.50$.

has the tetragonal chalcopyrite structure α at temperatures up to 625°C, above which it assumes the disordered zinc-blende β structure, while $MnIn_2Te_4$ is tetragonal $I\bar{4}2m$ (γ) at temperatures up to 630°C, above which it disorders to zinc-blend β. The zinc-blende β phase thus extends across the complete diagram and disappears in a eutectoid reaction at $z = 0.63$ and $T = 465$°C. In the L + δ field, the δ phase is a phase in the Ag_2Te–In_2Te_3 section, as shown previously (15). No DTA points were observed below the eutectoid temperature, indicating that the phase boundaries were very steep. However, the boundaries representing the limits of the α and γ fields at about 200°C were obtained from by the X-ray data; dashed lines being used to show these boundaries in Fig. 2.

Optical energy gap E_0 values were determined for all single-phase samples. Representative curves of $(\alpha h\nu)^2$ vs $h\nu$ for the alloys with $z = 0.20$ and 0.50 are shown in Fig. 3 and the resulting variation of E_0 with z is given in Fig. 4. Within the limits of experimental error, E_0 varies linearly with z in both single-phase fields, although the slope of the E_0 vs z line is different in the two cases. Straight line fits to the data in the two regions yielded

$$E_{0\alpha} = 0.961 + 0.55\ z\ (\text{eV}) \quad R = 0.995$$
$$E_{0\gamma} = 1.107 + 0.241\ z\ (\text{eV}) \quad R = 0.884.$$

As discussed below, E_0 varies quadratically with z in many cases. Ignoring the range of two-phase behavior, it is found that the fit to a quadratic equation yields

$$E_0 = 0.956 + 0.662\ z - 0.275\ z^2\ (\text{eV}) \quad R = 0.996,$$

which is perhaps a slightly better than that given by two straight lines.

DISCUSSION

As indicated in the Introduction, the limiting phases in this system are very similar; both are based on the zinc-blende subcell and are ordered to give a tetragonal lattice with $c/a \sim 2.0$. However, there is a change in the space group; $AgInTe_2$ has $I\bar{4}2d$ symmetry with $MnIn_2Te_4$ has $I\bar{4}2m$. Alloy systems containing Mn under similar conditions which have been investigated recently (8–10) have the form II_{1-z}–Mn_z–III_2–VI_4, e.g., $Cd_{1-z}Mn_zIn_2Te_4$ etc. In those cases, the space group changes from $I\bar{4}$ at $z = 0$ to $I\bar{4}2m$ at $z = 1$. It is of interest to compare the results for these latter alloys with the present data. For all three II_{1-z}–Mn_zIII_2–VI_4 systems, at room temperature and above, a single-phase solid solution is found across the complete composition range; the change in space group occurs at a particular composition, and results in a discontinuity in the phase boundary corresponding to the ordering temperature. Above this line, at $z = 1$, the structure is the completely disordered zinc-blende β phase but at $z = 0$, the structure is a partially ordered tetragonal form α_2'. The transition from α_2' to β occurs at the same composition as in the lower temperature case and results in a discontinuity in the solidus curve. One alloy system has discontinuity in the lattice parameter values, while another exhibits a discontinuity in E_0. No two-phase field has been observed at the change in space group, and if one occurs, it will be very narrow in z.

In the present system, the behavior is quite different. The two phases (α and γ) with different space groups are components in the eutectoid reaction involving the zinc-blende β phase, which extends across the complete diagram. A relatively wide two phase ($\alpha + \gamma$) field occurs, and there are no boundary discontinuities. The variations in lattice parameters and optical energy gap with z are divided into two separate sections, and within experimental limits can be considered as linear. However, it has been found in a wide range of alloys (17, 18) that the variation of E_0 with z is quadratic in form. If in the present case, the E_0 values for the two sections are treated together, it is found that the variation of E_0 with z can be

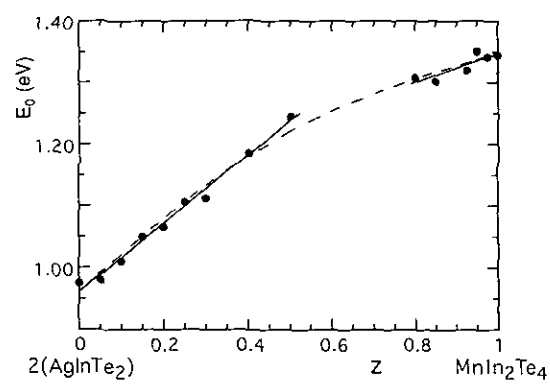

FIG. 4. Variation of optical energy gap E_0 with composition z for the $(AgIn)_{2(1-z)}(MnIn_2)_zTe_4$ alloys: (●) experimental values; (——) lines fitted to linear equations; (----) line fitted to quadratic equation.

fitted to a square-law form and that the fitted curve, quoted above, is slightly better than the linear fits. However, a similar fit can be made for the combined values of the lattice parameter a, giving

$$a = 0.6443 - 0.0169\,z - 0.0082\,z^2\,(\text{nm}) \quad R = 0.9994,$$

which is at least as good a fit as the separate linear ones given above. Thus with the present data, it is not possible to be more precise about the effects of change in space group on the values of a and E_0.

Thus, as far as the $T(z)$ diagrams are concerned, although for the two different alloy combinations the differences in the space groups appear comparable, the behavior of the alloy systems is very different.

ACKNOWLEDGMENTS

The authors are grateful to BID-CONOCIT (Project MN-09), CDCH-ULA, and CDCH-LUZ for financial support.

REFERENCES

1. J. K. Furdyna and J. Kossut, "Diluted Magnetic Semiconductors, Semiconductors and Semimetals," Vol. 25, Chap. 1., Academic Press, New York, 1989.
2. Y. Shapira, E. J. McNiff, Jr., N. F. Oliveira, Jr., E. D. Honig, K. Dwight, and A. Wold, *Phys. Rev. B* **37,** 411 (1988).
3. M. Quintero, E. Guerro, P. Grima, and J. C. Woolley, *J. Electrochem. Soc.* **136,** 1220 (1989).
4. C. Neal, J. C. Woolley, R. Tovar, and M. Quintero, *J. Phys. D: Appl. Phys.* **22,** 157 (1989).
5. M. Quintero, R. Tovar, H. Dhesi, and J. C. Woolley, *Phys. Status Solidi A* **115,** 157 (1989).
6. K.-J. Range and H.-J. Hübner, *Z. Naturforsch. B* **31,** 886 (1976).
7. G. Delgardo, C. Chacón, J. M. Delgado, and V. Sagredo, *Phys. Status Solidi A* **134,** 61 (1992).
8. E. Guerrero, M. Quintero, M. Delgardo, and J. C. Woolley, *Phys. Status Solidi A* **129,** K83 (1992).
9. E. Guerrero, M. Quintero, R. Tovar, T. Tinoco, J. González, and J. C. Woolley, *J. Electron Mat.* **22,** 297 (1993).
10. M. Morocoima, M. Quintero, and J. C. Woolley, *J. Solid State Chem.*, (in press).
11. J. C. Woolley, S. Bass, A.-M. Lamarche and G. Lamarche, *J. Mag. Mag. Mater.* **131,** 199 (1994).
12. M. Quintero, L. Dierker, and J. C. Woolley, *J. Solid State Chem.* **57,** 1911 (1986).
13. R. Chen and Y. Kirsh, "Analysis of Thermally Stimulated Processes, Internat. Series Science of Solid State," Vol. 15, p. 97. Pergamon Press, Elmsford, N.Y., 1981.
14. R. G. Goodchild, O. H. Hughes, S. A. López-Rivera, and J. C. Woolley, *Can. J. Phys.* **60,** 1096 (1982).
15. R. W. Chiang, D. F. O'Kane, and D. R. Mason, *J. Electrochem Soc.* **113,** 849 (1966).
16. M. Quintero, M. Morocoima, E. Guerrero, R. Tovar, M. Delgardo, and J. C. Woolley, *J. Cryst. Growth* **114,** 661 (1991).
17. J. A. Van Vechten and T. K. Bergstresser, *Phys. Rev. B.* **1,** 3351 (1970).
18. J. Avon, K. Yoodee and J. C. Woolley, *Nuovo Cimento Soc. Ital. Fis. D* **2,** 1858.11 (1983).